An NMR and Molecular Modeling Study of Carbosilane-Based Dendrimers Functionalized with Phenolic Groups or Titanium Complexes at the Periphery

Karen T. Welch,[b] Silvia Arévalo,[a] John F. C. Turner,*[b] and Rafael Gómez*[a]

Abstract: Dendrimers are modified polymers whose architecture is defined by the presence of a central atom or core with multiple branches. These molecules lend themselves to a variety of architectures and uses, including drug delivery and catalysis. The study of the molecular conformations and shapes of dendritic molecules is necessary but not yet routine. Here we present an NMR and molecular modeling study of a series of carbosilane dendrimers, namely 1G-{$(CH_2)_3[C_6H_3(OMe)]OH\}_4$ (**1**), 2G-{$(CH_2)_3[C_6H_3(OMe)]OH\}_8$ (**2**), and 2G-{$(CH_2)_3[C_6H_3(OMe)]O[Ti(C_5H_5)Cl_2]\}_8$ (**3**). Various two-dimensional NMR techniques were used to completely assign the ^1H and ^{13}C resonances of molecules **1**–**3**. This information was used, in conjunction with ^1H and ^{13}C spin-lattice relaxation measurements, to assess the chain motion of the molecules. The NMR data were also compared with 1-ns molecular dynamics (MD) simulations of **1** and **2** using the MMFF94 force field. The results indicate that these dendrimers possess a core that is motionally decoupled from the rest of the dendrimer, with flexible arm segments that extend from the core. The addition of eight functionalized titanium groups to the ends of the dendrimer chains of **2** to yield molecule **3** serves to further restrict chain motion.

Keywords: carbosilane · dendrimers · molecular dynamics · NMR spectroscopy · titanium

Introduction

Dendrimers are highly branched macromolecules with well-defined molecular weights and architectures, which provide unusual and novel properties that differentiate dendrimers from conventional polymers. Dendrimers are of great interest because of their potential application in various scientific disciplines, such as drug and gene delivery, unimolecular micelles, magnetic resonance imaging agents, and chemical sensors.[1] The use of dendritic molecules in catalysis has also received considerable attention.[2] The synthesis of dendritic molecules involves an iterative sequence of reaction steps in a convergent or divergent progression.[3] Dendrimers have four major architectural components, termed the core, branching, connector, and surface units, which allow the structure, size, shape, and functionality to be tuned to yield the desired physical and chemical properties; in principle, the synthetic procedures required to produce novel dendrimers are well established. However, information on the structural and conformational characterization of dendritic architectures has not kept pace with synthesis, though this information should allow a better understanding and prediction of the properties of new dendrimers. Proof of molecular structure can be determined by single-crystal X-ray diffraction studies; however, there are only a few examples of crystalline dendrimers, which, in general, are confined to low generations. This technique has therefore proved of little use so far.[4] For this reason, indirect techniques, such as nuclear magnetic resonance (NMR), matrix-assisted laser desorption/ionization time-of-flight (MALDI-TOF) and electrospray (ES) mass spectrometric methods, small-angle neutron (SANS) and X-ray (SAXS) scattering techniques, electron microscopy, and gel permation chromatography, have been used as analytical tools for the characterization of dendrimers. The determination of solid-state and solution con-

[a] Dr. S. Arévalo, Dr. R. Gómez
Departamento de Química Inorgánica
Universidad de Alcalá, Campus Universitario
E-28871, Alcalá de Henares (Spain)
Fax: (+34) 91-885-4683
E-mail: rafael.gomez@uah.es

[b] Dr. K. T. Welch, Dr. J. F. C. Turner
Department of Chemistry, 409 Buehler Hall
University of Tennessee, Knoxville Tennessee 37996-1600 (USA)
Fax: (+1) 865-974-3454
E-mail: jturner@atom.chem.utk.edu

Supporting information for this article is available on the WWW under http://www.chemeurj.org/ or from the author.

 DOI: 10.1002/chem.200400689

formations of dendritic molecules is not yet routine, and it is generally carried out by NMR and SANS techniques along with theoretical modeling and computer simulation. Moreover, the data generated to date affords contradicting predictions about the dendrimer packing and the maximum and minimum density inside the macromolecule.[5] For this reason, there is a need for more investigation of molecules with dendritic topology.

NMR is a powerful technique for the structural and conformational analysis of macromolecules, especially proteins. For dendrimers, not many studies have been carried out beyond the routine 1D NMR experiments, owing to the limited ability to resolve and assign the resonances of the chemically similar repeat units. However, multidimensional NMR experiments, in particular those based on inverse detection pulse sequences, offer the opportunity to obtain the complete structural characterization of the dendrimers by dispersing resonances into two or three dimensions when signals are overlapped in 1D NMR spectra. For instance, HMQC-TOCSY (heteronuclear multiple quantum coherence total correlation spectroscopy) 2D and 3D NMR experiments have been used for the complete assignment of the third generation poly-(propylene imine) dendrimer (DAB)[6]. A combination of 1D and 2D NMR techniques, including NOE (nuclear Overhauser enhancement) difference, EXSY (chemical exchange spectroscopy), COSY (correlation spectroscopy), and TOCSY, were employed for the characterization of cobalt(II) complexes of 2,6-diaminopyridine-containing dendrimers.[7] In the elucidation of dendrimer chain conformation by NMR, ^{1}H and ^{13}C NMR spin-lattice relaxation time (T_1) measurements along with 1D and 2D NOE experiments have been reported for a few examples of DAB,[6,8] poly(amidoamine) (PAMAM),[9] and polyether[10] dendrimers.

Only two NMR studies of silane dendrimers have been reported to date. The first used the 2D ^{29}Si–^{29}Si INADEQUATE (incredible natural abundance double quantum transfer experiment) experiment to confirm the structure of a first-generation polysilane dendrimer.[11] The second study, an impressive and challenging experiment based on 3D ^{1}H/^{13}C/^{29}Si triple resonance and pulsed field gradient (PFG) NMR techniques, characterized the structures of first- and second-generation hydride-terminated carbosilane dendrimers containing two-carbon-atom spacers.[12] A few studies concerning chain conformation have also been reported.[13]

Recently, we reported the synthesis of three-carbon spacer carbosilane dendrimers functionalized with phenols or titanium complexes at the periphery, and their characterization using routine 1D NMR experiments.[14] However, the chemical shift assignments for the methylene groups in the spacers were ambiguous, owing to the overlap of these resonances. In this paper, we describe a combination of 1D and 2D NMR experiments and the complete ^{1}H and ^{13}C assignments of the first and second generation of these dendrimers, in addition to information about their chain motion and conformation from T_1 measurements and molecular dynamics (MD) simulations.

Results and Discussion

Phenol-terminated carbosilane dendrimers: The first 1G-$\{(CH_2)_3[C_6H_3(OMe)]OH\}_4$ (**1**) and second 2G-$\{(CH_2)_3[C_6H_3(OMe)]OH\}_8$ (**2**) generations of three-carbon spacer carbosilane dendrimers functionalized with phenol groups at the periphery have been prepared using procedures analogous to those reported elsewhere.[14a] Briefly, these molecules were constructed in a divergent fashion by hydrosilylation reactions of the olefinic group of 4-allyl-2-methoxyphenol (eugenol) with the corresponding silicon hydride terminated dendrimers 2G-H_8 and 1G-H_4.[15] Figure 1 shows a representation of both dendrimers in which the methylene, methyl, and aromatic groups are labeled from the core to the exterior of the dendrimer.

*NMR characterization of 2G-$\{(CH_2)_3[C_6H_3(OMe)]OH\}_8$ (**2**)*: The 1D ^{1}H NMR spectrum was acquired at 600 MHz in [D_8]toluene. The spectrum can be divided into five regions with the methyl groups at about $\delta = 0.00$ ppm, the methylene groups at about $\delta = 0.70$–2.50 ppm, the methoxy group at $\delta = 3.30$ ppm, the hydroxy proton at $\delta = 5.80$ ppm, and the aromatic protons in the $\delta = 6.45$–6.90 ppm range (see Figure 2). From the relative intensities of the methyl resonances, it was possible to assign the inner methyl group Me_j and the outermost methyl groups Me_k to the signals at $\delta = 0.06$ and 0.00 ppm, respectively. Similarly, there are nine different sets of methylene protons, and because of the composition of the two generations, the intensities of the exterior methylene resonances (H_d–H_i) are double the intensities of the interior resonances (H_a–H_c). Within the methylene groups, we can predict three different sets of resonances based upon their respective chemical environments. The farthest upfield resonances were those of the five methylene groups adjacent to silicon atoms. Moving downfield, the next group of resonances were those corresponding to the three central methylene groups of the three-carbon spacers. Finally, the resonance of the benzylic methylene group was the farthest downfield and unique in chemical shift. The methylene groups of the innermost branch could be further identified by the lower intensity of these resonances.

Two-dimensional homonuclear and heteronuclear NMR experiments were required to complete the assignment of 2G-$\{(CH_2)_3[C_6H_3(OMe)]OH\}_8$ (**2**). It was evident from the TOCSY spectrum that there were three isolated spin systems consisting of three sets of methylene protons each. Figure 3 shows the TOCSY spectrum recorded for **2** at a mixing time of 40 ms. The assignment proceeded by identification of the three spin systems by means of the TOCSY and COSY spectra, followed by differentiation of the resonances adjacent to silicon atoms using HMBC (heteronuclear multiple-bond correlation), and confirmation of the assignments with the NOESY (nuclear Overhauser effect spectroscopy) spectra. The outermost spin system (resonances H_g, H_h, and H_i) was identified by the presence of the benzylic protons. This resonance, H_i, had two cross peaks at $\delta = 1.59$ for H_h and 0.54 ppm for H_g. The middle branch

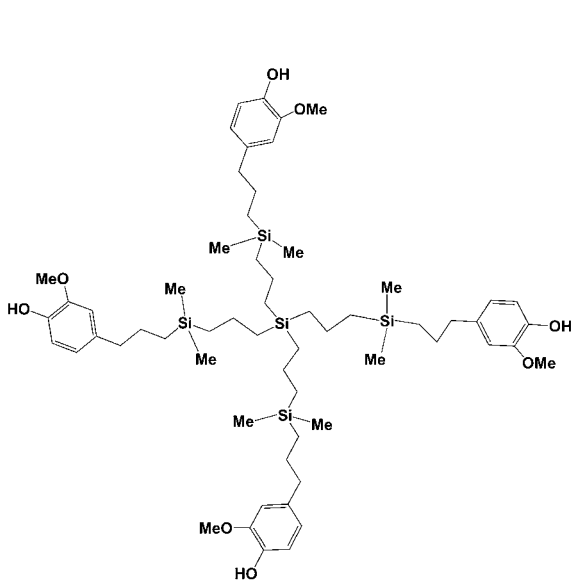

1G-[$(CH_2)_3${C_6H_3(OMe)}OH]$_4$ (**1**)

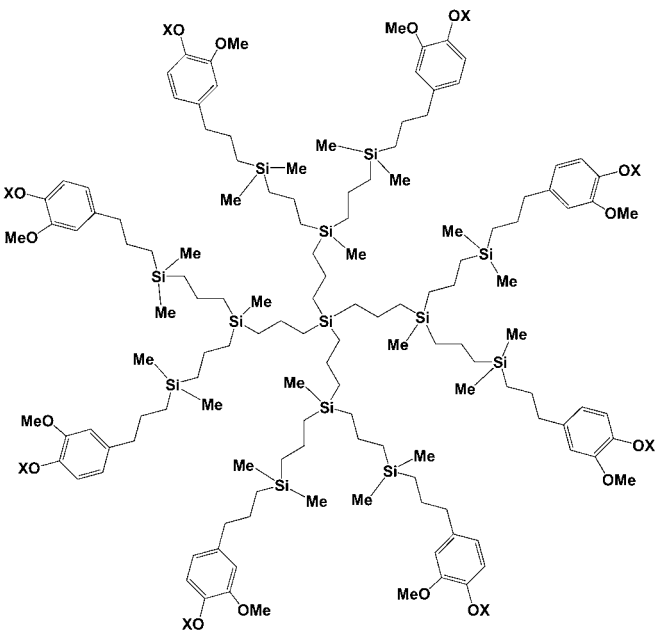

2G-[$(CH_2)_3${C_6H_3(OMe)}OX]$_8$; X = H (**2**), [Ti(C_5H_5)Cl_2] (**3**)

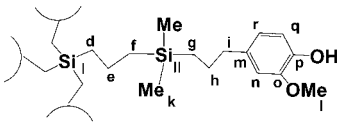

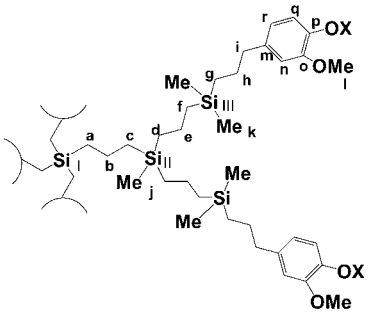

Figure 1. Molecular representation of the first-, 1G-{$(CH_2)_3[C_6H_3(OMe)]OH\}_4$ (**1**), and second-generation, 2G-{$(CH_2)_3[C_6H_3(OMe)]OH\}_8$ (**2**) and 2G-{$(CH_2)_3[C_6H_3(OMe)]O[Ti(C_5H_5)Cl_2]\}_8$ (**3**), dendrimers with branches labeled from the core to the exterior of the dendrimer.

resonances, H_d, H_e, and H_f, were identified by their relative intensities, and produced three strong TOCSY crosspeaks at $\delta = 1.45$, 0.68, and 0.62 ppm. The farthest downfield signal at $\delta = 1.45$ ppm was attributed to H_e as the methylene group not adjacent to silicon. Resonances H_d and H_f, were differentiated by the HMBC data, in which H_d showed connectivity to Me_j and H_f was connected to Me_k. These assignments were also supported by the NOESY data, as there was a NOESY crosspeak between the methyl group of the outer silicon atom (Me_k) and the methylene protons H_f and H_g. For the interior methylene branch, a weaker TOCSY correlation was detected, as was expected given their relative abundance. Hence, the signal at $\delta = 1.57$ ppm was due to H_b and the peaks at $\delta = 0.78$ and 0.71 ppm were attributed to H_a and H_c indistinctly. No NOE cross peaks were observed between the inner methyl group (Me_j) and H_c. Because of this, and only in this case, tentative assignments were made. Based on the trend of increasing chemical shift towards the core of the dendrimer (see below) and the analogy in the surroundings between H_c and H_d, the peak at $\delta = 0.71$ ppm was assigned to H_c and the peak at $\delta = 0.78$ ppm was assigned to H_a. In the case of the aromatic protons, the TOCSY and NOESY spectra permit assignment of the signals at $\delta = 6.59$ and 6.87 ppm as H_r and H_q, respectively. The assignment of the H_r resonance was supported by an NOE between the H_r and H_i resonances. For the signal at $\delta = 6.47$ ppm, no TOCSY correlation is shown and due to H_n and confirmed by NOE with H_i.

The 150.9 MHz 1D ^{13}C NMR spectrum of **2** in [D_8]toluene is shown in Figure 2. Inverse detection 2D {^1H–^{13}C} HSQC (heteronuclear single-quantum coherence) and HMBC experiments were used in assigning the carbon atom resonances. The cross peaks observed in the HSQC spectrum at $\delta = 40.19$, 26.90, and 15.66 ppm were attributed to the outer methylene groups, H_i/C_i, H_h/C_h, and H_g/C_g, respectively, on the basis of the proton assignments, and were verified by the HMBC experiment. The region of the spectrum in which the inner and middle methylene ^{13}C resonances were

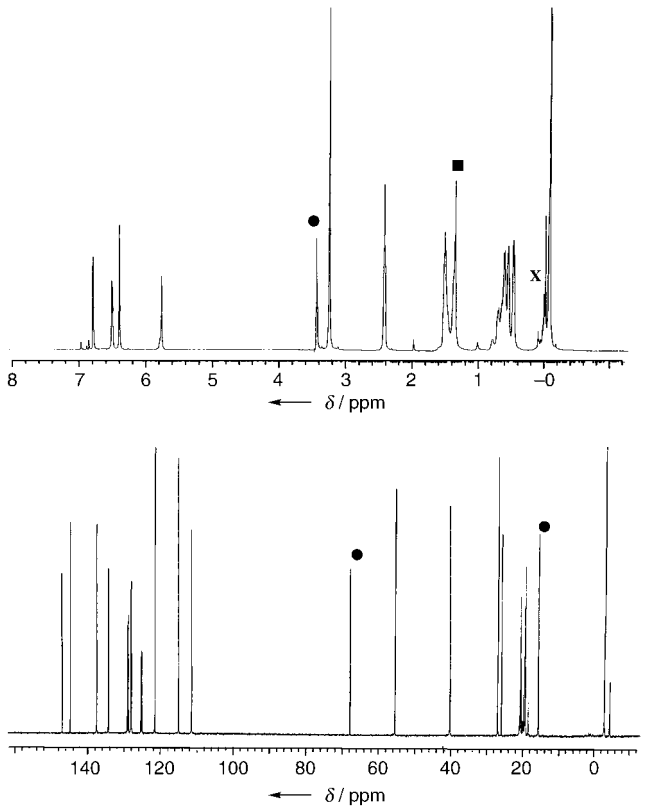

Figure 2. 1D ^{1}H NMR (600 MHz, $[D_8]$toluene) and 1D $^{13}C\{^{1}H\}$ NMR (150.8 MHz, $[D_8]$toluene) spectra of 2G-$\{(CH_2)_3[C_6H_3(OMe)]OH\}_8$ (**2**). Peak labeled with a circle (●) is from THF impurity; peak labeled with a square (■) denotes signal overlapped with THF impurity; peak labeled with the symbol (**X**) denotes an impurity.

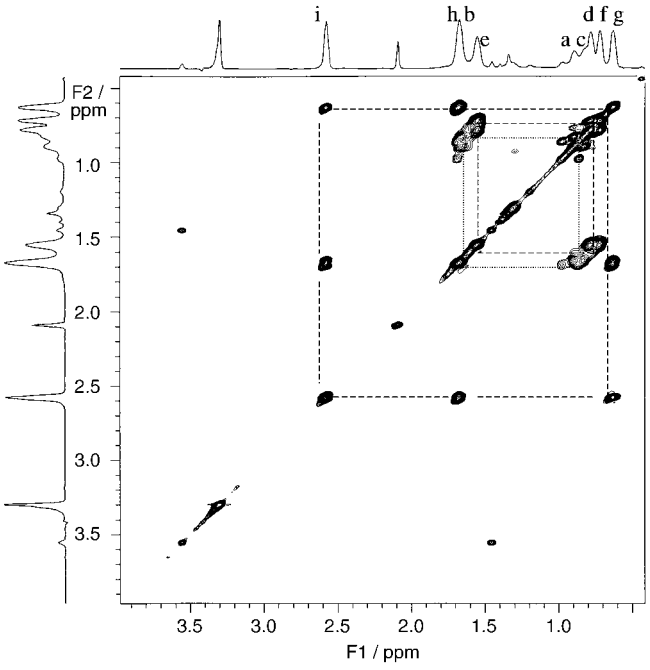

Figure 3. 2D $\{^{1}H\text{-}^{1}H\}$ TOCSY NMR (600 MHz, $[D_8]$toluene) spectrum of 2G-$\{(CH_2)_3[C_6H_3(OMe)]OH\}_8$ (**2**) in the methylene and methyl regions.

found was complicated by overlap with the residual toluene solvent resonances. However, from the 2D $\{^{1}H\text{-}^{13}C\}$ HSQC spectrum, the cross peaks C/H at $\delta = 19.17/1.45$, 19.34/0.68, and 20.58/0.62 ppm were assigned to C_e, C_d, and C_f respectively. The 2D $\{^{1}H\text{-}^{13}C\}$ HMBC spectrum supported these assignments, the H_e proton signal showed two cross peaks to C_d and C_f, which in turn showed cross peaks to Me_j and Me_k, respectively. For the innermost three-carbon spacer group, the cross peak at $\delta = 19.43/1.57$ ppm, observed in the HSQC spectrum, was assigned to C_b/H_b; it showed two cross peaks of decreased intensity (with respect to those shown for the middle and outer methylene spin systems) in the HMBC spectrum, owing to the connectivity with C_a and C_c. The assignments of the individual resonances C_a and C_c were attributed to the signals at $\delta = 19.82$ and 18.41 ppm, respectively, from the HSQC spectrum and based on the proton assignments. The HMBC spectrum showed a cross peak between the Me_j protons and C_c that partially overlaps with the more intense cross peak Me_j/C_d, which established the assignment more unambiguously. Figure 4 shows the 2D $\{^{1}H\text{-}^{13}C\}$ HSQC NMR spectrum of 2G-$\{(CH_2)_3[C_6H_3(O\text{-}Me)]OH\}_8$ (**2**) in the methylene and methyl regions. The 2D $\{^{1}H\text{-}^{13}C\}$ HSQC and HMBC experiments allowed for facile confirmation of the assignments of the aromatic carbon resonances.

If the 1D ^{1}H NMR spectrum was acquired in $[D_1]$chloroform, the chemical shifts of the methylene resonances adjacent to silicon in the dendritic structure were observed to overlap. A similar behavior was found in the ^{29}Si NMR spectra of **2**, in which, in $[D_8]$toluene, three different silicon resonances were observed; in contrast, in $[D_1]$chloroform the innermost silicon atom was never detected.[14a,16] These features are consistent with the observations of Rinaldi et al. who proposed a model in which chloroform migrates into the core of the dendrimer, solvating all of the methylene groups, whereas toluene does not solvate the interior of the dendrimer molecule.[6] In further agreement with this idea, in toluene, protons H_a, H_c, H_d, H_f, and H_g, with almost identical chemical environments, have chemical shifts of $\delta = 0.78$, 0.71, 0.68, 0.62, and 0.54 ppm, respectively, showing gradual upfield shifts on going from the core to the surface. This feature is consistent with a progressively greater interaction with the anisotropic toluene solvent when protons are closer to the surface of the molecule. In addition, this conclusion would confirm the previous and tentative assignment for H_a/C_a and H_c/C_c under the supposition of similar surroundings.

*NMR characterization of 1G-$\{(CH_2)_3[C_6H_3(OMe)]OH\}_4$ (**1**)*: The first-generation dendrimer **1** presented 1D ^{1}H and ^{13}C NMR spectra that were considerably simpler than those of compound **2** because of the nonexponential growth of the dendrimer chains. However, this system served to confirm the second-generation structural assignments described above. The proton and carbon signals of the inner and outer methylene groups were easily identifiable by using 2D TOCSY, HSQC, and HMBC spectra. The TOCSY experi-

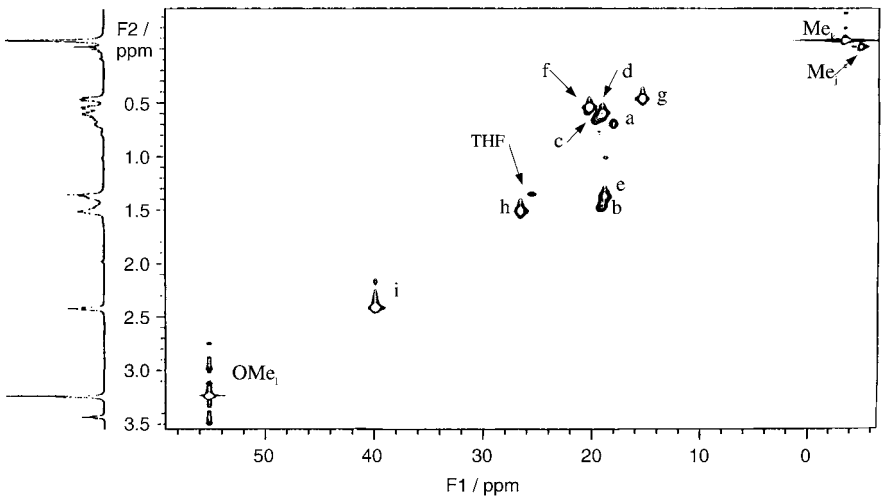

Figure 4. 2D {^{1}H-^{13}C} HSQC NMR spectrum of 2G-{$(CH_2)_3[C_6H_3(OMe)]OH\}_8$ (**2**) in the methylene and methyl regions.

ments demonstrated the connectivity of the H_g, H_h, and H_i resonances. The triplet at $\delta = 2.55$ ppm, which was ascribed to the benzylic protons H_i, in analogy to the observations from the second-generation dendrimer **2**, gave two cross peaks at $\delta = 1.65$ ppm, attributed to the middle methylene group H_h, and $\delta = 0.60$ ppm corresponding to the Si−CH_2 groups (H_g). The resonance at $\delta = 1.54$ ppm was assigned to H_e as its environment was similar to H_h, and it gave two overlapped cross peaks owing to its connectivity with H_d and H_f. From the TOCSY experiment alone, it was not possible to differentiate H_d and H_f. However, we can discriminate them easily from the 2D NOESY, HSQC, and HMBC combination spectra (see below), attributing the resonances at $\delta = 0.76$ ppm to H_d and $\delta = 0.68$ ppm to H_f. These assignments were in agreement with those for the inner methylene branch of the dendrimer **2**. The HSQC spectrum showed clearly resolved C/H correlations for the CH_2 groups, allowing us to attribute the resonances at $\delta = 40.20$, 26.89, 19.30, and 15.65 ppm to the carbon atoms C_i, C_h, C_e, and C_g respectively, based on the proton assignments. The signal at $\delta = 20.71$ ppm was assigned to C_f, whereas that at $\delta = 18.15$ ppm corresponded to C_d carbon atom, based on the data inferred in the HMBC spectrum. The resonance at $\delta = 0.68$ ppm and attributed to H_f had a long distance C/H correlation with the methyl groups Me_k.

In the case of the aromatic proton and carbon atoms, their assignments are in agreement with those of the second-generation dendrimer **2**. The ^{1}H and ^{13}C chemical shift assignments for **1** and **2** are summarized in Table 1.

Titanium phenoxide terminated carbosilane dendrimers: The second generation 2G-{$(CH_2)_3[C_6H_3(OMe)]O$-$[Ti(C_5H_5)Cl_2]\}_8$ (**3**) was prepared from the phenol-terminated carbosilane dendrimer **2** by reaction with $[Ti(C_5H_5)Cl_3]$ to liberate HCl using the procedure previously described.[14a]

Table 1. ^{1}H and ^{13}C NMR chemical shift assignments for dendrimers **1**–**3**.[a]

	δ(^{1}H)			δ(^{13}C)		
Assignment	**1**	**2**	**3**	**1**	**2**	**3**
methylene						
a	–	0.78	0.75	–	18.41	18.31
b	–	1.57	1.53	–	19.43	19.31
c	–	0.71	0.70	–	19.82	19.72
d	0.76	0.68	0.68	18.15	19.34	19.30
e	1.54	1.45	1.45	19.30	19.17	19.08
f	0.68	0.62	0.63	20.71	20.58	20.47
g	0.60	0.54	0.56	15.65	15.66	15.70
h	1.65	1.59	1.60	26.89	26.90	26.62
i	2.55	2.50	2.52	40.20	40.19	40.26
methyl						
j	–	0.06	0.06	–	−4.51	−4.47
k	0.00	0.00	0.02	−3.04	-2.96	−2.91
l	3.38	3.31	3.47	55.30	55.40	56.18
aryloxy						
m	–	–	–	134.39	134.35	139.93
n	6.49	6.47	6.58	111.23	111.42	113.42
o	–	–	–	146.84	146.99	150.24
p	–	–	–	144.63	144.76	157.63
q	6.93	6.87	6.82	114.80	114.96	119.30
r	6.63	6.59	6.53	121.51	121.51	120.63
X = OH, C_5H_5	5.42	5.81	6.27	–	–	121.01

[a] Data from 600 MHz in [D_8]toluene at room temperature and using 160 mM dendrimer concentration.

The 1D ^{1}H and ^{13}C NMR spectra were acquired using the same conditions as for **1** and **2**, and showed almost identical chemical shifts for the carbosilane backbone resonances. The resonances of the aromatic proton and carbon atoms were slightly shifted, as expected for the replacement of the phenolic hydroxyl group with a $[OTi(C_5H_5)Cl_2]$ fragment. The most relevant feature was the observation of well-separated chemical shifts for H_b and H_h, at $\delta = 1.53$ and 1.60 ppm respectively, in contrast to the overlapping resonances observed for the analogous positions in **2.** The complete atomic connectivities and ^{1}H and ^{13}C chemical shifts assignments for **3** were thus determined and are summarized in Table 1.

Molecular modeling and solution behavior of phenol- and titanium-terminated dendrimers 1–3: Models of the 1G (**1**) and 2G (**2**) dendrimers were constructed to visualize their dynamic or motional behavior. The objective of the model study was to determine the influence of the dendrimer architecture on the motion of the individual "arms" or chains. Molecular dynamics was performed on the two molecules for one nanosecond. For the MD trajectories of **1** and **2**, distances and angles were measured at points along each arm to assess local motion. For the 1G dendrimer, there were one set of Si–Si distances, one set of CH_2–CH_2 distances, one set of Si–CH_2–Si angles, and one set of CH_2–Si–CH_2 angles. For the 2G dendrimer, there were two sets of Si–Si distances and two sets of CH_2–CH_2 distances as well as angles, and these could be differentiated as "inner" and "outer" distances depending on the distance from the core of the dendron. In addition, the distances between all 1,3-Si–CH_2 units were measured. These distances were consistent for both molecules **1** and **2**, therefore either the X–X distances or the X–Y–X angles could be used to represent the conformational state of each chain segment.

Based on the data in Table 2, there were subtle differences between the two molecules. The average Si_I–Si_{II} distance for the 1G dendrimer was 5.72 Å, whereas the interior Si_I–Si_{II} distance for the 2G dendrimer was 5.76 Å, and the exterior Si_{II}–Si_{III} distance was 5.72 Å. These values indicate that the two segments were nearly fully extended, and that the model predicts greater flexibility around the silicon atoms. Examination of the CH_2–CH_2 distances for molecules **1** and **2** revealed a greater difference between the exterior CH_{2e}–CH_{2h} units of molecule **2** and the other two sets of methylene groups. For the 1G and 2G interior methylene units, the average distance is about 4.5 Å, whereas the same distance for the exterior methylene units is about 4.7 Å. Both segments fluctuate about a conformation that is approximately 1 Å short of full extension.

When the dynamics trajectories of each of the structural units were plotted as distances or angles versus time, the existence of persistent local chain conformations, or local minima, was apparent (Figure 5). For the Si–Si unit, there were two populated regions around 132° and 172° (Si–CH_2–Si angle). The number of transitions from one conformational well to the other was dependent upon the structure of the molecule as well as the relative position of the structural unit within the molecule.

The interpretation of the dynamics trajectories for the CH_2–CH_2 units was not as straightforward because of the greater apparent flexibility of these units, as evidenced by larger oscillations about the persistent local chain conformers, as well as a greater number of local conformers. There are four local chain minima located around 80–88°, 102°, 118°, and 160°, with the regions around 80–88° and 118° more heavily populated (CH_2–Si–CH_2 angle). The trends in conformational transitions were analogous to the Si–Si unit. Thus, the model predicted a gradual slowing of chain motion upon the accumulation of successive generations.

The molecular dynamics simulations also yielded information about the shapes of molecules **1** and **2**. The cores of both molecules can be described as spheres with radii of about 5.7 Å, in which the first shell of four silicon atoms is on the surface of the sphere. The structure of the core is roughly tetrahedral with a distance of 9.1 ± 1.5 Å between pairs of silicon atoms. Thus, the core portion of the molecules loosely retains the geometry of the central silicon atom, although there are some deviations with the 1 ns dynamics trajectories. For both molecules, the exterior chains of the molecule oscillate in the conformational space between an extended state and a folded state, in which they appear to be loosely wrapped around the core. The phenolic chain termini at times extend to within 4.4–4.6 Å of the central silicon atom, although these chain conformations were present less than 10% of the time for all segments of the molecules (see Tables 3 and 4). Thus, the phenolic end groups are not significant contributors to density in the cores of the molecules, suggesting that the interaction of chains on the periphery of the molecule serves to rigidify

Table 2. Distance and angle data for simulated dendrimers **1** and **2**.

Dendrimer	Atom pair	Distance [Å]	Angle [°]
1	Si_I–Si_{II}	5.72 ± 0.23	159.15 ± 18.03
1	CH_2–CH_2	4.53 ± 0.59	102.91 ± 19.91
1	1,3-CH_2–Si[a]	2.94 ± 0.07	–[b]
2	Si_I–Si_{II}(interior)	5.76 ± 0.21	162.22 ± 16.07
2	Si_I–Si_{II}(exterior)	5.72 ± 0.23	159.59 ± 17.93
2	CH_2–CH_2 (interior)	4.54 ± 0.63	103.65 ± 21.67
2	CH_2–CH_2 (exterior)	4.69 ± 0.59	108.51 ± 20.76
2	1,3-CH_2–Si[a]	2.94 ± 0.07	–[b]

[a] Represents the average distance for all contiguous 1,3-CH_2–Si units in the molecule. [b] This value was not measured.

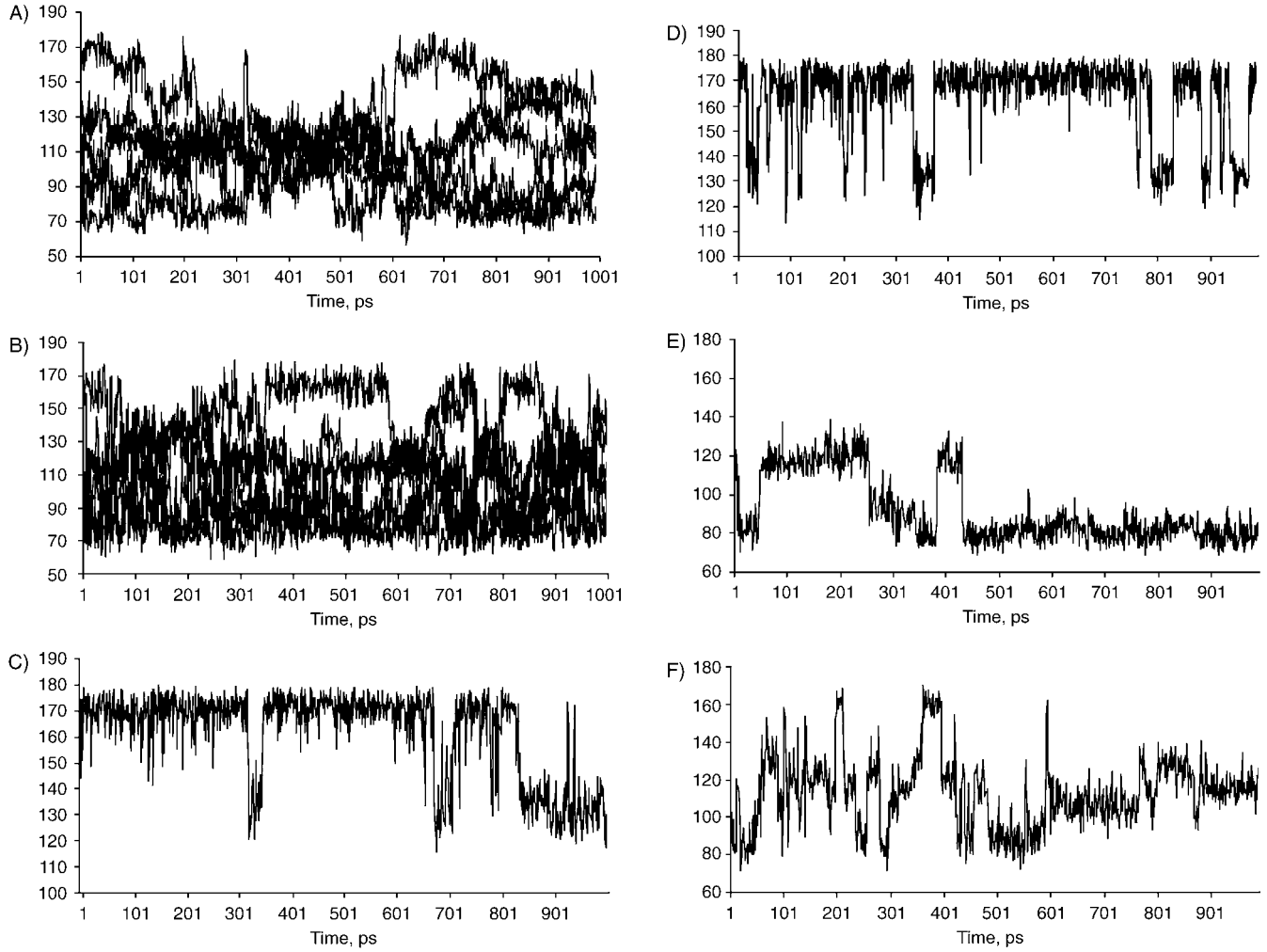

Figure 5. Molecular modeling data of **1** and **2** for one nanosecond: A) **2**, angle trajectories Si_{II}–Si_{I}–Si_{II}. B) **1**, angle trajectories Si_{II}–Si_{I}–Si_{II}; C) **2**, angle trajectory Si_{I}–CH_{2b}–Si_{II} (interior Si–Si unit); D) **2**, angle trajectory Si_{II}–CH_{2h}–Si_{III} (exterior Si–Si unit); E) **2**, angle trajectory CH_{2b}–Si_{II}–CH_{2e} (interior CH_2–CH_2 unit); F) **2**, angle trajectory CH_{2e}–Si_{II}–CH_{2h} (exterior CH_2–CH_2 unit).

Table 3. Data pertaining to core structure and backfolding of dendrimers **1** and **2**.

Measurement	Atoms	**1**	**2**
angle [°]	Si_{II}–Si_{I}–$Si_{II'}$	107.86 ± 26.70	108.08 ± 23.71
distance [Å]	Si_{I}–Si_{II}	8.99 ± 1.46	9.12 ± 1.32
	Si_{I}–C_{m}	7.85 ± 1.27	9.45 ± 2.45
	Si_{I}–O_{p}	9.55 ± 2.35	11.10 ± 3.27
	Si_{I}–Me_{1}	9.37 ± 2.19	10.90 ± 3.04

Table 4. Backfolding analysis of dendrimers **1** and **2**.

Atom pair	**1**, < 5.8 Å	**2**, < 5.8 Å
Si_{I}–C_{m}	2.1 %	2.4 %
Si_{I}–O_{p}	5.0 %	6.1 %
Si_{I}–Me_{1}	6.1 %	6.2 %

the interior. Figure 6 shows a picture of dendrimer **2** at 190 ps time in the dynamic trajectory.

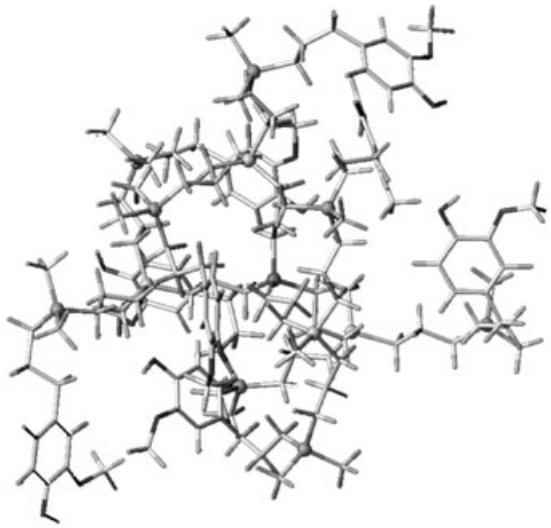

Figure 6. Molecular modeling of dendrimer **2** at 190 ps time in the dynamic trajectory.

Once all the proton and carbon resonances of the dendrimers were fully assigned, it was possible to investigate their solution behavior with ^1H and ^{13}C spin-lattice relaxation time (T_1) measurements. Correlation of the relaxation behavior of the resonances with their local environments can be used to gain information about the relative density distribution within the macromolecule.[17] Relaxation parameters were obtained for dendrimers **1**–**3**, using [D_8]toluene as a solvent and at 600 MHz, by inversion-recovery experiments (recorded in Table 5). Figure 7 shows the ^1H T_1 values for the methylene and methyl groups of the three dendritic macromolecules. For the second-generation dendrimer **2**, the topologically interior protons have T_1 values slightly lower than those observed for the middle and outer methylene protons. These features suggest that the interior nuclei reside in a region of slower average molecular motion. The ^1H T_1 data for the two different Me–Si groups are consistent with this trend as well. The observation of greater freedom of motion on going from inner to terminal methylene and methyl groups might suggest a radial decrease in density of the macromolecule and a less congested local environment in the periphery than in the core. This finding fits the model of Lescanec and Nuthukumar,[18] which predicts a monotonic decrease in density on going from the center to the periphery of the dendrimers. However, this behavior is opposite to that found in polyether dendrimers by Frechet and co-workers[10c] or by Veggel and co-workers;[10d] this was in agreement with the de Gennes and Hervet simplified model,[19] which places a density maximum at the periphery of the dendrimers. The ^1H T_1 values for **2** were also determined as a function of the concentration (see Figure 8). The T_1 values of the inner methylene and methyl groups were not sensitive to changes in concentration, in contrast to the rest of the resonances in the macromolecule. This invariance could be attributed to a closer packing of the molecules at higher concentrations, which does not affect the motion in the interior of the molecule. The T_1 values for the dendrimer exterior groups were concentration-dependent; when the concentration of the solution was decreased, the ^1H T_1 values increased. These results also support the above hypothesis of different frequencies of motion for the inner and outer fragments. In addition, plotting the T_1 data versus concentration gives information about the correlation time (τ) regime. For the inner groups, the invariance could be attributed to nuclei with τ near to the minimum in the plot of ^1H T_1 versus τ. However, the exterior groups would behave on the low side of the T_1 minimum.

^{13}C T_1 experiments were also performed to investigate molecular motion. Examination of these relaxation values revealed behavior analogous to that found in ^1H NMR T_1 experiments (see Figure 7). A comparison of the ^1H and ^{13}C T_1 values of the three-carbon spacer units for both the second and first generations showed lower values with increasing generation, thus suggesting less free motion in the interior of the molecule, as expected.

The relaxation data for dendrimer **3** are shown in Table 5. One of the most notable differences in the relaxation data of **2** and **3** was the dramatic shortening of ^1H and ^{13}C T_1 values for the outermost methylene groups and the terminal phenoxide fragment. The shorter relaxation times found for **3** could be ascribed either to a molecular conformation that reduced the segmental motion, as the [$Ti(C_5H_5)Cl_2$] group

Table 5. ^1H and ^{13}C NMR spin-lattice relaxation times (T_1) of dendrimers **1**–**3**.[a]

	^1H (T_1)			^{13}C (T_1)		
Assignment	**1**	**2**	**3**	**1**	**2**	**3**
methylene						
a	–	0.54	0.55	–	0.28	0.24
b	–	0.60[b]	0.54	–	0.37	0.35[e]
c	–	0.56	0.52[d]	–	0.31	0.30
d	0.57	0.60	0.52[d]	0.41	0.40	0.35[e]
e	0.63	0.68	0.55	0.58	0.56	0.46
f	0.70	0.69	0.53	–[c]	0.55	1.15[c]
g	0.74	0.67	0.43	0.72	0.60	0.37
h	0.74	0.66[b]	0.42	0.77	0.65	0.38
i	0.81	0.71	0.39	0.72	0.60	0.33
methyl						
j	–	1.01	0.84	–	1.64	1.16
k	1.44	1.28	0.79	–	–	–
l	1.87	1.59	0.41	–	–	1.09
aryloxy						
m	–	–	–	–	–	0.87
n	2.30	1.82	0.47	1.28	0.99	0.42
o	–	–	–	–	–	–
p	–	–	–	–	–	–
q	3.72	3.22	0.93	1.14	1.00	0.41
r	2.49	2.04	0.67	1.25	0.90	0.42
X = OH, C_5H_5	2.19	4.81	1.24	–	–	1.38

[a] Data from 600 MHz in [D_8] toluene at room temperature and using 6 mM dendrimer concentration. [b] Partial overlapping of signals H_b and H_h. [c] Overlapping with the toluene signals. [d] Partial overlap of signals H_c and H_d. [e] Overlap of signals C_b and C_d.

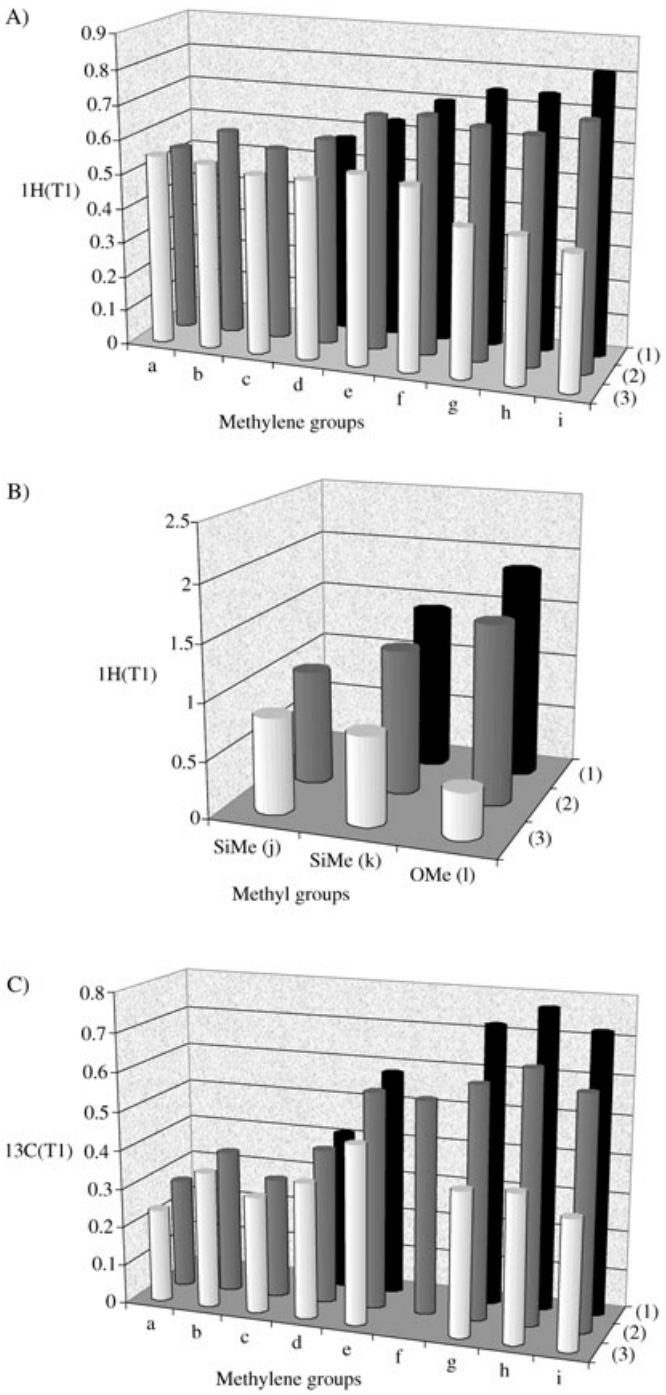

Figure 7. ^{1}H and ^{13}C spin-lattice relaxation time (T_1) data of **1**–**3** for the methylene and methyl groups, using 600 MHz in [D_8]toluene, room temperature and 160 mM dendrimer concentration. A) ^{1}H (T_1) methylene groups; B) ^{1}H (T_1) methyl groups; C) ^{13}C (T_1) methylene groups.

tends to anchor the chain, or to an aggregation process of the dendrimer in these conditions.[8b] However, for the innermost methylene branch, the T_1 values suggested no change in the motional behavior as compared with **2**.

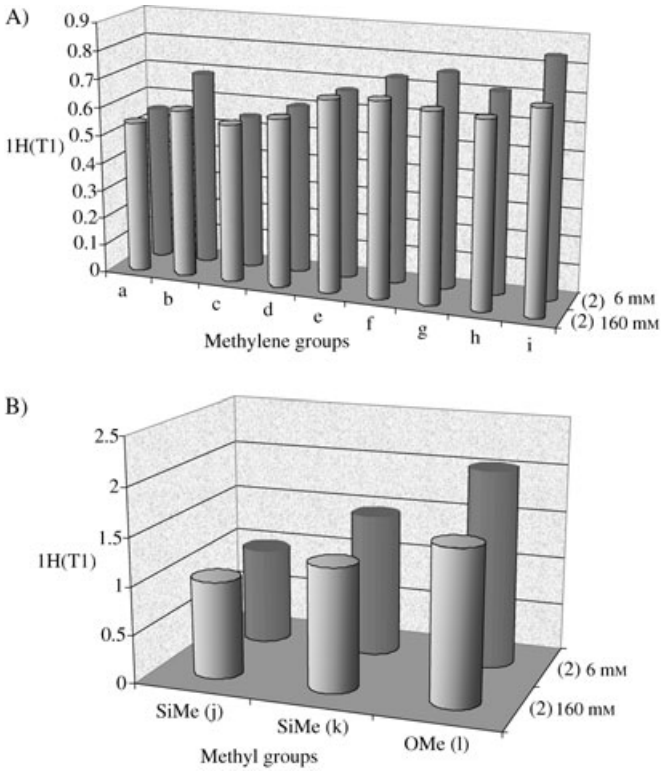

Figure 8. ^{1}H spin-lattice relaxation time (T_1) data of **2** for the methylene and methyl groups, using 600 MHz in [D_8]toluene, room temperature and 160 and 6 mM dendrimer concentrations. A) methylene groups; B) methyl groups.

Conclusion

In the work presented here, we have fully assigned the proton and carbon resonances of first- and second-generation phenol-terminated carbosilane dendrimers and the second generation of the analogous titanium-ended carbosilane dendrimer, using a combination of 1D (^{1}H, $^{13}C\{^{1}H\}$) and 2D (COSY, TOCSY, HSQC, HMBC, and NOESY) NMR spectroscopic techniques. These assignments were based on the well resolved signals that occur in [D_8]toluene as solvent. The assignments allowed us to obtain information about the molecular motion and conformation by measuring the ^{1}H and ^{13}C spin lattice relaxation times (T_1). These data were consistent with a somewhat rigid, spherical core conformation for the carbosilane dendrimers functionalized by terminal phenolic groups, as was predicted by the molecular dynamics calculations. In addition, the molecular models were consistent with a looser periphery of flexible chains that was affected by changes in dendrimer concentration, as was determined experimentally for **2**.

The NMR evidence also suggests a further slowing of molecular motion or conformational exchange within the dendrimer molecule caused by the addition of the [$CpTiCl_2$] moiety. The mass of this group is analogous to one layer of nonexponential growth of the polymer, a single $C_{12}H_{19}O_2Si$ unit per arm. This is evident in the decrease of the T_1 values for resonances g, h, and i in molecules **2** and **3**. Since the

large, somewhat spherical surface area of the [$CpTiCl_2$] groups is less favorable for interchain associations by van der Waals interactions, the molecular mass of this group is likely to be the cause of the change.

We note that the [$CpTiCl_2$] moieties reside in the periphery of the dendrimer and that **3** represents an intermediate stage between a purely homogenous Ziegler–Natta precatalyst and a precatalyst that has been heterogenized in the sense of both the steric encumberance around the catalyst and the composition of the coordination sphere of the Ti atom. We are currently exploring this effect on the catalytic activity of this and related systems.

Experimental Section

Materials: The carbosilane dendrimers 1G-{$(CH_2)_3[C_6H_3(OMe)]OH\}_4$ (**1**), 2G-{$(CH_2)_3[C_6H_3(OMe)]OH\}_8$ (**2**), and 2G-{$(CH_2)_3[C_6H_3(OMe)]O$-$[Ti(C_5H_5)Cl_2]\}_8$ (**3**) (see structures in Figure 1) were synthesized according to reference [14a]. Deuterated solvents [D_8]toluene and [D_1]chloroform were purchased from Cambridge Isotope Laboratory (Andover, MA). Deuterated toluene was dried over potassium and distilled before use. All dendrimers were pumped before use and the preparation of the samples was performed in the glove box under argon. All solutions were degassed by several freeze-pump-thaw cycles in 5 mm Young's tap NMR tubes. The samples were prepared in two different concentrations (160 mM and 6 mM).

NMR measurements and data processing: All of the NMR data were acquired on a 300 MHz Varian Mercury spectrometer or a Varian INOVA 600 spectrometer equipped with VNMR 6.1B software. All processing of NMR data was perfomed with the standard Varian software. The 2D-NMR data were processed using a forward linear prediction and weighted using either a gaussian or sinebell apodization function prior to Fourier transfomation. For the HSQC and HMBC experiments, $^1J_{C,H}$ = 120 Hz and $^xJ_{C,H}$ = 8 Hz. The T_1 experiments were set up and analysed using the dot1 macro available within the VNMR 6.1B software package. A relaxation delay of 12–16 s was used in the ^{1}H NMR experiments and a relaxation delay of 8 s was used in the ^{13}C NMR experiments.

Molecular modeling: The MMFF94 forcefield as implemented in Sybyl 6.9 was used for all calculations. MMFF 94 was first published by Halgren in 1995, and was parameterized for simulations of organic molecules and proteins.[20] Of the forcefields available within the Sybyl 6.9 software package (Tripos Inc., 1699 South Hanley Rd., St. Louis, MO, 63144, USA), it performed best in maintaining a tetrahedral geometry about the silicon atoms, and in carrying out the molecular dynamics simulations. The models used in the simulations were constructed with the Builder module of Sybyl 6.9. The models were built incrementally with successive cycles of simulated annealing and minimization to yield a reasonable starting structure for molecular dynamics simulations. The MD simulations were carried out at 300 K for 1 ns and a timestep of 1 fs. Structures were saved every 1000 fs, and the first 10 ps of the simulation were used for equilibration. In all calculations, solvent was treated implicitly with a dielectric constant of 2.3 debye. Visualization of the resulting trajectories was also carried out with Sybyl 6.9.

Acknowledgement

We acknowledge the Ministerio de Ciencia y Tecnología (Project BQU2001-1160) and Comunidad Autónoma de Madrid (Project 07N/0078/2001) for financial support. R.G.R. is grateful to the Secretaría de Estado de Educación y Universidades of the Government of Spain for providing a fellowship (ref. PR2001-0050). K.T.W. acknowledges the University of Tennesee for funding. The Varian^{INOVA} 600 was purchased with funding from the University of Tennessee, and the Varian Mercury 300 was purchased with funding from Eastman Chemical Co. and the University of Tennessee. J.F.C.T. is grateful to the University of Tennessee for provision of start-up funds.

[1] a) M. Fischer, F. Vögtle, *Angew. Chem.* **1999**, *111*, 934–955; *Angew. Chem. Int. Ed.* **1999**, *38*, 884–905, and references therein; b) *Dendrimers and other dendritic polymers* (Eds.: J. M. Fréchet, D. A. Tomalia), Wiley Series in Polymer Science, Wiley, **2001**; c) *Dendrimers and Dendrons: Concepts, Syntheses, Applications* (Eds.: G. R. Newkome, C. N. Moorefield, F. Vögtle), Wiley-VCH, **2001**.

[2] a) D. Astruc, F. Chardac, *Chem. Rev.* **2001**, *101*, 2991–3023; b) G. E. Oosterom, J. N. H. Reek, P. C. J. Kamer, P. W. N. M. van Leeuwen, *Angew. Chem.* **2001**, *113*, 1878–1901; *Angew. Chem. Int. Ed.* **2001**, *40*, 1828–1849; c) G. E. Oosterom, S. Steffens, J. N. H. Reek, P. C. J. Kamer, P. W. N. M. van Leeuwen, *Top. Catal.* **2002**, *19*, 61–73.

[3] a) C. N. Moorefield, G. R. Newkome in *Advances in Dendritic Macromolecules, Vol. 1* (Ed.: G. R. Newkome), Jai Press Inc., London, **1994**, pp. 1–67; b) O. A. Matthews, A. N. Shipway, J. F. Stoddart, *Prog. Polym. Sci.* **1998**, *23*, 1–56.

[4] a) A. W. Bosman, M. J. Bruining, H. Kooijman, A. L. Spek, R. A. Janssen, E. W. Meijer, *J. Am. Chem. Soc.* **1998**, *120*, 8547–8548; b) J.-P. Mayoral, A.-M. Caminade, *Chem. Rev.* **1999**, *99*, 845–880, and references therein; c) P. I. Coupar, P. A. Jaffrés, R. E. Morris, *J. Chem. Soc. Dalton Trans.* **1999**, 2183–2187; d) H. Schumann, B. C. Wassermann, M. Frackowiak, B. Omotowa, S. Schutte, J. Velder, S. H. Mühle, W. Krause, *J. Organomet. Chem.* **2000**, *609*, 189–195.

[5] A. W. Bosman, H. M. Janssen, E. W. Weijer, *Chem. Rev.* **1999**, *99*, 1665–1688.

[6] M. Chai, Y. Niu, W. J. Youngs, P. L. Rinaldi, *J. Am. Chem. Soc.* **2001**, *123*, 4670–4678.

[7] a) J. D. Epperson, L. J. Ming, B. D. Woosley, G. R. Baker, G. R. Newkome, *Inorg. Chem.* **1999**, *38*, 4498–4502; b) J. D. Epperson, L. J. Ming, G. R. Baker, G. R. Newkome, *J. Am. Chem. Soc.* **2001**, *123*, 8583–8592.

[8] a) J. F. G. A. Jansen, E. M. M. De Brabander-van der Berg, E. W. Meijer, *Science* **1994**, *265*, 1226–1229; b) Y. Pan, W. T. Ford, *Macromolecules* **1999**, *32*, 5468–5470; c) Y. Pan, W. T. Ford, *Macromolecules* **2000**, *33*, 3731–3738.

[9] A. D. Meltzer, D. A. Tirrell, A. A. Jones, P. T. Inglefield, D. M. Hedstrand, D. A. Tomalia, *Macromolecules* **1992**, *25*, 4541–4548.

[10] a) C. B. Gorman, M. W. Hager, B. L. Parkhurst, J. C. Smith, *Macromolecules* **1998**, *31*, 815–822; b) D. L. Jiang, T. Aida, *J. Am. Chem. Soc.* **1998**, *120*, 10895–10901; c) S. Hecht, J. M. Fréchet, *J. Am. Chem. Soc.* **1999**, *121*, 4084–4085; d) H. J. van Manen, R. H. Fokkens, N. M. M. Nibbering, F. C. J. M. van Veggel, D. N. Reinhoudt, *J. Org. Chem.* **2001**, *66*, 4643–4650.

[11] J. B. Lambert, E. Basso, N. Qing, S. H. Lim, J. L. Pflug, *J. Organomet. Chem.* **1998**, *554*, 113–116.

[12] M. Chai, Z. Pi, C. Tessier, P. L Rinaldi, *J. Am. Chem. Soc.* **1999**, *121*, 273–279.

[13] a) M. A. Mazo, P. A. Zhilin, E. B. Gusarova, S. S. Sheiko, N. K. Balabaev, *J. Mol. Liq.* **1999**, *82*, 105–116; b) X. Khang, K. T. Haxton, L. Ropartz, D. J. Cole-Hamilton, R. Morris, *J. Chem. Soc. Dalton Trans.* **2001**, 3261–3268; c) M. Elshakre, A. S. Atallah, S. Santos, S. Grigoras, *Comput. Theor. Polym. Sci.* **2001**, *10*, 21–28.

[14] a) S. Arevalo, J. M. Benito, E. de Jesús, F. J. de la Mata, J. C. Flores, R. Gómez, *J. Organomet. Chem.* **2000**, *602*, 208–210; b) S. Arevalo, E. de Jesús, F. J. de la Mata, J. C. Flores, R. Gómez, *Organometallics* **2001**, *20*, 2583–2592; c) S. Arevalo, E. de Jesús, F. J. de la Mata, J. C. Flores, R. Gómez, M. P. Gómez-Sal, P. Ortega, S. Vigo, *Organometallics* **2003**, *22*, 5109–5113.

[15] Synthetic procedure analogous to: D. Seyferth, D. Y. Son, A. L. Rheingold, R. L. Ostrander, *Organometallics* **1994**, *13*, 2682–2890.

[16] The ^{29}Si NMR chemical shift for the second-generation dendrimer 2G-{$(CH_2)_3[C_6H_3(OMe)]OH\}_8$ (**2**) measured in [D_8]toluene: δ = 1.04 (core Si), 1.34 (intermediate Si), and 1.82 ppm (outermost Si).

[17] a) W. J. Chazin, L. D. Colebrook, *Magn. Reson. Chem.* **1985**, *121*, 4084–4085; b) Y. Tomoyose, D. L. Jiang, R. H. Jin, T. Aida, T. Yamashita, K. Horie, *Macromolecules* **1996** *29*, 5236–5238; c) D. L. Jiang, T. Aida, *Nature* **1997** *388*, 454–456.
[18] R. L. Lescanec, M. Muthukumar, *Macromolecules* **1990**, *23*, 2280–2288.
[19] P. G. de Gennes, H. Hervet, *J. Phys. Lett.* **1983**, *44*, L351-L360.
[20] T. A. Halgren, *J. Comput. Chem.* **1996**, *17*, 490–519; T. A. Halgren, *J. Comput. Chem.* **1996**, *17*, 520–552; T. A. Halgren, *J. Comput. Chem.* **1996**, *17*, 553–586; T. A. Halgren, *J. Comput. Chem.* **1996**, *17*, 587–615; T. A. Halgren, *J. Comput. Chem.* **1996**, *17*, 616–641.

Received: September 8, 2004
Published online: January 11, 2005

